Accepted Manuscript

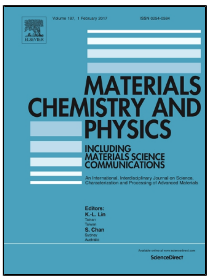

Superior Mechanical Properties of Poly Vinyl Alcohol-Assisted ZnO Nanoparticle Reinforced Epoxy Composites

Sudipta Halder, Tankeshwar Prasad, Nazrul Islam Khan, M.S. Goyat, Sri Ram Chauhan

PII:	S0254-0584(16)30968-3
DOI:	10.1016/j.matchemphys.2016.12.055
Reference:	MAC 19386
To appear in:	*Materials Chemistry and Physics*
Received Date:	03 August 2016
Revised Date:	11 December 2016
Accepted Date:	27 December 2016

Please cite this article as: Sudipta Halder, Tankeshwar Prasad, Nazrul Islam Khan, M.S. Goyat, Sri Ram Chauhan, Superior Mechanical Properties of Poly Vinyl Alcohol-Assisted ZnO Nanoparticle Reinforced Epoxy Composites, *Materials Chemistry and Physics* (2016), doi: 10.1016/j.matchemphys.2016.12.055

Highlights

- PVA-assisted ZnO modification was done by sol-gel method to control their particle size
- Average particle size of ~62 nm with uniform nanorods like structures was achieved
- Enhancement in T_g value of epoxy system suggests strong interfacial interactions with fillers
- Significant improvement in mechanical properties was obtained at 2 wt.% filler content

Superior Mechanical Properties of Poly Vinyl Alcohol-Assisted ZnO Nanoparticle Reinforced Epoxy Composites

Sudipta Halder[a*], Tankeshwar Prasad[a], Nazrul Islam Khan[a], M.S. Goyat[b], Sri Ram Chauhan[a]

[a] Department of Mechanical Engineering, National Institute of Technology Silchar, Silchar-788010, Assam, India

[b]Department of Physics, College of Engineering Studies, University of Petroleum & Energy Studies, Dehradun, Uttarakhand, 248007, India

*Author to whom correspondence should be addressed. E-mail: sudiptomec@gmail.com, Fax: +91-3842-224797

Abstract

This work demonstrates the effect of poly vinyl alcohol modified ZnO nanoparticles on thermal and mechanical properties of epoxy nanocomposites. Modified ZnO nanoparticles with controlled particle size were successfully synthesized by sol-gel method. The surface modification of nanoparticles was confirmed by FT-IR, EDX and TGA analysis. Epoxy nanocomposites were prepared using different wt.% (0-3 wt.%) of unmodified and modified ZnO nanoparticles. A significant improvement in T_g was achieved for synthesized epoxy nanocomposites. The dispersion and interfacial interactions between unmodified (ZN) and PVA modified ZnO (PZN) with the epoxy matrix were investigated by morphological study of fractured surface of epoxy nanocomposites. The improvement in mechanical performance of PVA-assisted ZnO nanoparticle reinforced epoxy composites was found superior at 2 wt.% of particle concentration. The maximum enhancement in mechanical properties such as tensile strength, tensile modulus, compressive strength, flexural strength and flexural modulus was ~24, 47, 48, 44 and 77% respectively with respect to that of neat epoxy system. We have exposed the potential of the PVA-assisted ZnO nanoparticle as good choice of reinforcement for composite industries.

Key Words: ZnO nanoparticles; Fracture toughness; Thermal stability; Mechanical testing; Sol-gel method

1. Introduction

Over the past few years, the introduction of nanoparticles (NPs) such as carbon, metallic or inorganic particles into polymer matrices led to significant improvement in thermal, mechanical and electrical properties of the

nanocomposite [1-5]. However, another option is the incorporation of low-cost micron sized particles into polymers which can stiffen and increase the strength of the material under certain loading conditions. But, the use of micron sized particles in these days is not so common due to generation of some other undesirable properties [6]. Therefore, worldwide research is going on to modify polymer matrices using different nano-fillers. In these days, low-cost and abundant ZnO nanoparticles are in great demand because of its morphological diversity, controlled particle size and crystalline structure. These characteristics of ZnO nanoparticles have a significant effect on the property improvement not only for semiconductors, solar cells, gas sensors, paints, cosmetics, catalysts and varistors [7-9], but also for other applications [10]. This enriches the motivation to scientists with regard to the special characteristics and morphology of ZnO nanoparticles to scrutinize not only its properties but also approaches to develop technically less sensitive and cost effective processing routes [11]. Over the past few years, the nanosized ZnO as ceramic filler has been widely used in the field of high strength polymer composites [12], electronic glass (ceramics), high-density polyethylene include safety helmets and stadium seating, as it can improve mechanical performance and thermal resistance properties of the polymers [13-15]. But, all types of pristine nanoparticles are very prone to aggregate in viscous polymers due to their high surface area and energy, which results in poor thermal and mechanical properties of the nanocomposites. Thus, to yield a better compatibility between the nano-fillers and the polymer matrix, the use of particle surface modification by various techniques is recommended to enhance the desired properties of nanocomposites [16-19]. It is already well-established that the surface modification of nano-fillers has been a convenient method to reduce the surface energy of nanoparticles while improving its dispersion to achieve required performance characteristics of nanocomposites [20]. The modified surface of nanoparticles is more reactive for the miscibility of the nanofillers into the viscous polymer matrices [21-23]. Recently, the preparations of ZnO/epoxy composites with homogeneous dispersion were reported by Ding et al. [22]. The investigation showed that the composite containing 5 wt% of ZnO particles (about 100–200 nm) had the optimal mechanical properties. The addition of ZnO nanoparticles into the epoxy matrix resulted in a significant increment in the thermal stability and activation energy of thermal degradation. The epoxy nanocomposite exhibited an increase in storage modulus and glass transition temperature compared to the neat epoxy. Rashmi R. Devi et al. [23] reported the vinyl trichlorosilane (VTCS) modified ZnO nanoparticles based Wood polymer nanocomposite. The mechanical properties including modulus of rupture (MOR), tensile strength, hardness, and thermal stability were studied. They found considerable amount of properties enhancement with uniformly dispersed nano-ZnO particles in the polymer

matrices. Mallakpour et al. [24] reported the modification of ZnO nanoparticles using poly vinyl alcohol (PVA) to increase the compatibility and dispersibility in the PVC matrix. They reported, some improvement in tensile strength, strain, and elongation at break about 27%, 19%, and 19% respectively at high filler content of 8 and 12 wt.%. In another work, Xie et al. [25] reported the surface modification of nano-Sb_2O_3 by polymethyl methacrylate (PMMA) and its effect on mechanical properties of Sb_2O_3/PVC nanocomposites. They showed the improvement in dispersibility of particles in the matrix as well as improvement in stiffness and strength of the matrix at 2.5 wt.% of filler content. Chatterjee et al. [26] investigated the effect of nano-calcium carbonate ($CaCO_3$) containing PMMA nanoparticles on thermal and mechanical properties of polypropylene (PP) composites. Their results showed the homogeneous dispersion of $CaCO_3$ nanoparticles in PP matrix due to grafting with PMMA and also significant enhancement of thermal and mechanical properties were observed at 1 wt.% filler content in the matrix.

In the above context, study on the effect of surface modified ZnO nanoparticles on thermal and mechanical properties of epoxy resin system has been reported for the first time. In this study, we focused on the homogeneous dispersion of ZnO nanoparticles and their impact on the thermal and mechanical properties of the resulting composites. However, earlier reported studies based on ZnO nanofillers reinforced polymers reveal only nanofiller dispersion and interfacial interactions as the two main issues governing the properties of nanocomposites [27, 28]. Most of the literatures reported the functionalization of commercially available ZnO nanoparticles by attaching non-covalent functional groups on their surfaces, but such kind of functionalization produces poor interfacial adhesion between ZnO particles and polymer matrix leading to insignificant enhancement in mechanical properties. To achieve a desired set of properties in polymer nanocomposites, adopting a suitable method capable of controlling the interfacial interaction is of quite important. Therefore, in the present study, ZnO nanofillers were functionalized with PVA through sol-gel method and then reinforced them into polymer matrix to enhance the interfacial interaction between the filler and matrix. The effects of unmodified and PVA-assisted ZnO nanoparticles on the thermal and mechanical properties of epoxy nanocomposites with respect to varied filler concentration were investigated. The possible toughening mechanisms were identified by microscopic investigation of the fractured surfaces of nanocomposites.

2. Experimental

2.1 Materials

Zinc Sulfate heptahydrate ($ZnSO_4•7H_2O$) used as a precursor and sodium hydroxide (NaOH) as a reagent were supplied by Merck specialties private ltd, Mumbai, India. Poly vinyl alcohol (PVA), ER grade (MW: 22,000 g/mol) was used as a capping agent and purchased from Loba chemie private ltd., Chennai, India. Diglycidylether of bisphenol-A (DGEBA) based epoxy resin (Lapox L12) with density 1.20 g cm^{-3} and Triethylenetetramine, (TETA, K6) hardener with density 0.95 g cm^{-3} were supplied by Atul ltd., Gujarat, India.

2.2. Surface modification of ZnO nanoparticles

Surface modification of ZnO nanoparticles was carried out by using sol-gel method. Initially, $ZnSO_4•7H_2O$ and NaOH were mixed in a molar ratio of 1:2 and dissolved in deionized water to obtain an aqueous solution. Further, 0.28 g of PVA (equivalent to 10 wt.% PVA in $ZnSO_4$) was added to 10 ml of deionized water. Then, continuous stirring was employed at 60 °C for 25 min to achieve a homogenous solution. The resultant solution was mixed with zinc solution under continuous stirring followed by drop wise addition of NaOH solution. The reaction was carried out for approximately 3 h till the formation of white precipitate. The white precipitate was centrifuged, washed and dried in vacuum at 80 °C for 12 h. The resultant dried material was grounded to fine powder using agate mortar. Finally, the powder was calcined for 2 h at 500 °C. The ZnO nanoparticles modified with 10 wt.% PVA in $ZnSO_4$ are designated as PZN. Using the same method, unmodified ZnO nanoparticles were synthesized but without using PVA and designated as ZN. The possible reaction mechanism between PVA monomer and hydroxyl groups of ZnO nanoparticle is illustrated in Scheme-1.

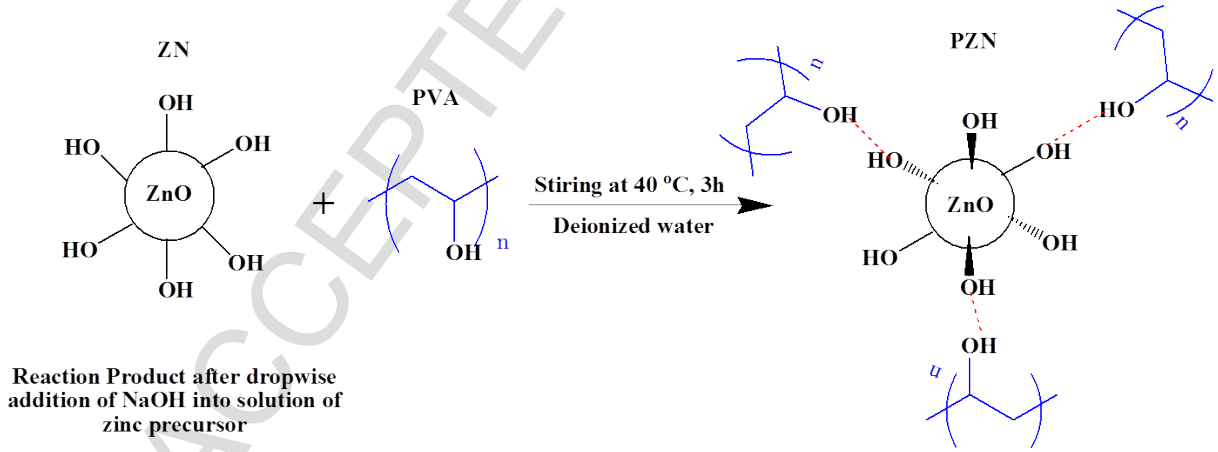

Scheme 1: Schematic representation of reaction mechanism between PVA monomer and hydroxyl groups of ZnO nanoparticles.

2.3. Preparation of ZnO/epoxy nanocomposites

Varying amount of unmodified and PVA modified ZnO nanoparticles (1, 2 and 3 wt.%) was chosen for preparation of ZnO/epoxy nanocomposites. High shear mixing was used for blending of the nanoparticles into the epoxy network. Initially, the nanoparticles suspended epoxy resin was continuously stirred at 2000 rpm for 15 min. Later, in a stoichiometric ratio, hardener was added to the ZnO/epoxy resin mixture under continuous stirring for 5 min at 400 rpm. Thereafter, the resulting mixture was sonicated in an ultrasonic bath for 25 min to obtain homogenous mixture. After the ultrasonication, the mixture was degassed at room temperature to remove the entrapped air bubbles. Finally, the mixture was poured into rubber molds followed by pre-curing at room temperature for 24 h and post-curing at 80 ^{o}C for 2 h to obtain different sets of cured samples. For ease in writing, the neat epoxy is designated as NE, unmodified and PVA modified ZnO/epoxy nanocomposites consisting 1, 2 and 3 wt.% of ZnO are designated as (ZEC-1, ZEC-2 and ZEC-3) and (PZEC-1, PZEC-2 and PZEC-3) respectively.

2.4. Characterization

Morphology, particle size and particle size distribution of nanoparticles were investigated using FESEM, (Zeiss, model: Supra 55VP, Germany). Chemical characterization was done by FTIR spectrometer (Bruker, model: Hyperion Microscope with Vertex 80, Germany) to identify surface functional groups of modified ZnO nanoparticles. The structural properties of the synthesized nanoparticles were investigated by powder X-ray diffractometer (XRD), (Phillips, model: X'Pert PRO diffractometer, USA) with Cu Kα-radiation and energy dispersive X-ray (EDX) analysis (Zeiss, model: Supra 55VP, Germany). Glass transition temperature and thermal decomposition behavior of samples were measured using a simultaneous thermal analyzer i.e. simultaneous application of Thermogravimetry (TGA) and Differential Scanning Calorimetry (DSC) (NETZSCH, model: STA 449F3, Germany). The analysis was performed on 10 mg of samples in a temperature range of 50 to 800 ºC with a heating rate of 20 ºC/min under nitrogen gas purging. The mechanical properties such as tensile, compression and flexural strength were determined using a computerized universal tensile machine (INSTRON, Model 8801, USA). The tensile properties of samples were investigated according to ASTM D 638 (type-V) standard. The compression tests were conducted in accordance to ASTM D695-96 with specimen size (cube) of 12.5 x 12.5 x 12.5 mm^3 and the flexural properties from single edge notched bending (SENB) specimen were investigated according to ASTM D5045 with specimen size of 53 x 12 x 6 mm^3. All SENB specimens were tapped by a sharp razor blade to create sharp cracks of ~ 6 mm length. At least five specimens were tested for each composition and property. The tensile

and SENB test fracture specimens were examined under FESEM to investigate the toughening mechanisms of ZnO/epoxy nanocomposites.

3. Results and discussion

3.1. PVA-assisted growth mechanism of ZnO nanoparticles

During sol-gel process, the growth of pristine ZnO nanoparticles generally follows the diffusion-limited Ostwald ripening mechanism. But, in presence of capping agent (PVA), the growth of nanoparticles follows a combination of diffusion and surface reaction mechanism [29]. This can be explained on the basis of Scheme-1. During the hydrolysis process, the increase in zinc precursor concentration significantly increases the nucleation rate of ZnO, which results in formation of large amount of ZnO nuclei due to the decomposition of intermediate parts of $Zn(OH)_2$ precipitates. On the other hand, at a constant pH (10), some of $Zn(OH)_2$ precipitates may have transformed into the growth units of $[Zn(OH)4]^{2-}$ due to alkaline condition. It is well-known that the polar growth of ZnO nano-crystal along (0001) direction proceeds through the adsorption of growth units of $[Zn(OH)4]^{2-}$ onto (0001) plane. These grown nuclei may aggregate together due to excess saturation [30]. There is a possibility of ionic–dipolar interaction due to electrostatic force between PVA and the growth units along the crystal plane (0001), which may lead to the formation of nucleus of rod-like twinning crystal. The growth of the individual crystallite in a twin crystal occurs along the polar c-axis due to incorporation of growth units on the growth interface plane (0001), which possess highest surface energy in nature and thus leads to the formation of rod-like ZnO nano-crystals [31].

3.2. Morphology of ZnO nanoparticles

Fig. 1(a-b) shows the FESEM images of unmodified and modified ZnO nanoparticles, which clearly reveal varying particle size, their size distribution and change in morphologies. The average particle size of unmodified and modified ZnO nanostructures was determined from FESEM image in terms of aspect ratio using Image J software. The average particle size of unmodified ZnO nanoparticles was ~78 nm (aspect ratio: 5.38) with mixed morphology of nanorod and nanoflakes like structures (Fig. 1a). But, the modified ZnO reveals the average particle size ~62 nm (aspect ratio: 4.53) with uniform nanorod like structures (Fig. 1b and Fig. 2a). Fig. 2(b) shows the histrograms of particle size distribution of unmodified ZnO nanoparticle (ZN) and PVA modified ZnO nanoparticle (PZN). Generally, the use of capping agent during the synthesis of nanoparticles plays a vital role in controlling the particle size and its morphology [32].

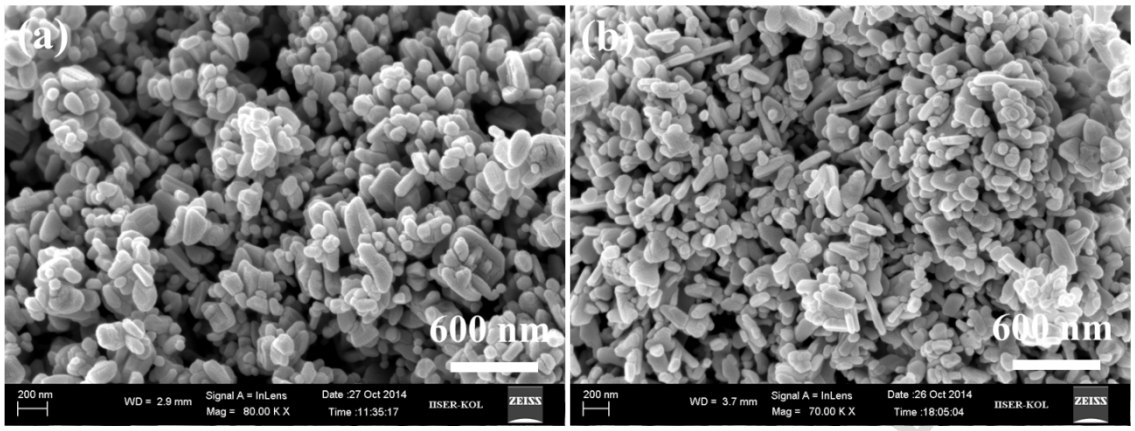

Fig. 1 Morphology of (a) unmodified ZnO nanoparticle (ZN) and (b) PVA modified ZnO nanoparticles (PZN).

However, in absence of any capping agent, there is no control over the nucleation and growth of nanocrystals and which may lead to the rapid growth of the nanoparticles without allowing any phase separation. This may lead to anisotropic growth of the nanostructures along any direction. Also, the surface of nanostructure is quite unstable which leads to the formation of irregular shape and size (Fig. 1a), in order to attain its normalized surface energy [33]. But, when the capping agent is introduced during synthesis, then the synthesized ZnO nanostructures exhibit well-developed facet planes. The variations in the morphology may affect the crystallinity of the material because of controlled growth rate of nanostructures in presence of the capping agent is possible [34-37].

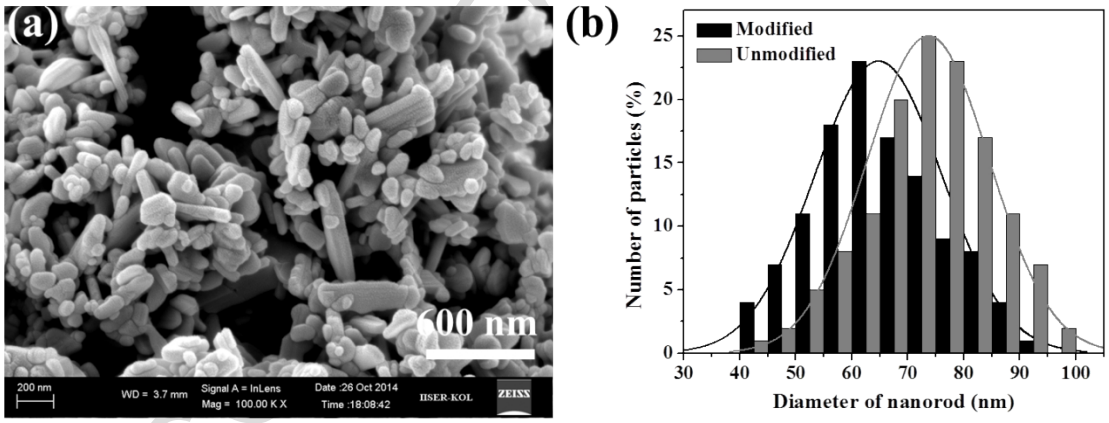

Fig. 2 (a) Morphology of modified ZnO nanoparticle at high magnification (b) histogram of particle size distribution of Unmodified ZnO nanoparticle (ZN) and PVA modified ZnO nanoparticle (PZN).

3.3. Structural property of ZnO nanoparticles

Fig. 3 shows the FT-IR spectra of unmodified ZnO nanoparticles (ZN) and modified ZnO nanoparticles (PZN). The spectra of ZN reveal a broad peak at 472 cm^{-1}, which is a characteristic absorbance peak of ZnO. Another band at

3500 cm^{-1} is attributed to the presence of hydroxyl groups (–OH) on the surface of ZnO nanoparticles. However, from the spectra of PZNs, peaks at 1430 cm^{-1} and 1326 cm^{-1} represent C-C stretching and C-H deformation vibrations, respectively. The C-O stretching and O-H bending vibrations of the PVA chains were detected by the absorption peaks at 1100 cm^{-1} [38]. Thus, the spectra of PZNs reveal characteristic peaks of both ZnO and hydroxyl group from PVA, which confirms the successful surface modification of ZnO.

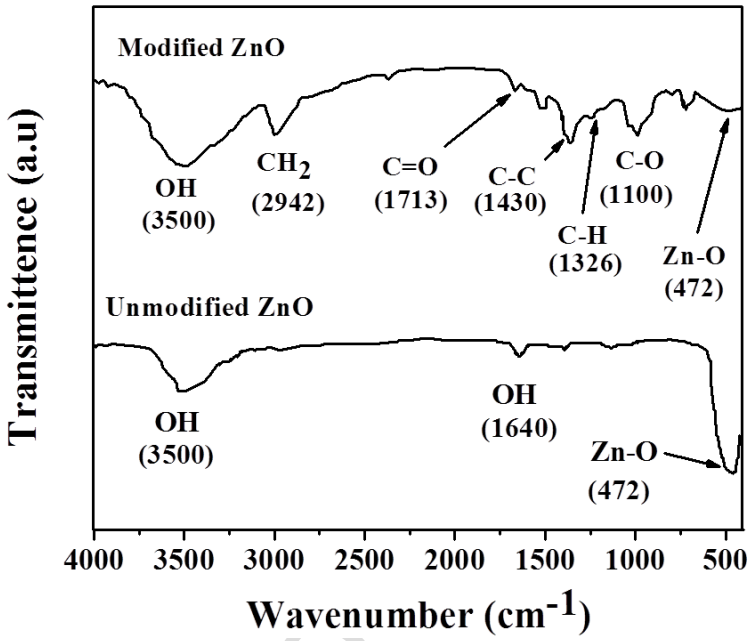

Fig. 3 FTIR spectra of Unmodified ZnO nanoparticle (ZN) and PVA Modified ZnO nanoparticle (PZN).

Fig. 4 shows the TGA curves of unmodified (ZN) and unmodified ZnO (PZN). As reflected by the TGA curves, weight loss occurs in two steps for PZN while no such behavior is observed for ZN. Initial weight loss at 50 °C is attributed to the removal of the physically absorbed volatile solvents and moisture absorbed on the surface of hydrophilic PVA chains in PZN.

Table. 1 Elemental analysis of unmodified and PVA modified ZnO nanoparticles from EDX spectra.

Unmodified ZnO			**Modified ZnO**		
Element	**Weight %**	**Atomic %**	**Element**	**Weight %**	**Atomic %**
C K	-	-	C K	9.16	18.35
O K	29.96	63.71	O K	41.22	61.96
Zn K	70.04	36.29	Zn K	49.62	19.69
Total	100		Total	100	

In second step, rapid weight loss between 200 and 400 °C may be attributed to dehydration process of hydroxyl groups from PVA chains and formation of oxides. A noticeable weight loss about 5.30% is observed in case of PZNs. This may be due to presence of PVA on the surface of nanoparticles, which again confirms the successful functionalization of the surface of ZnO nanoparticles.

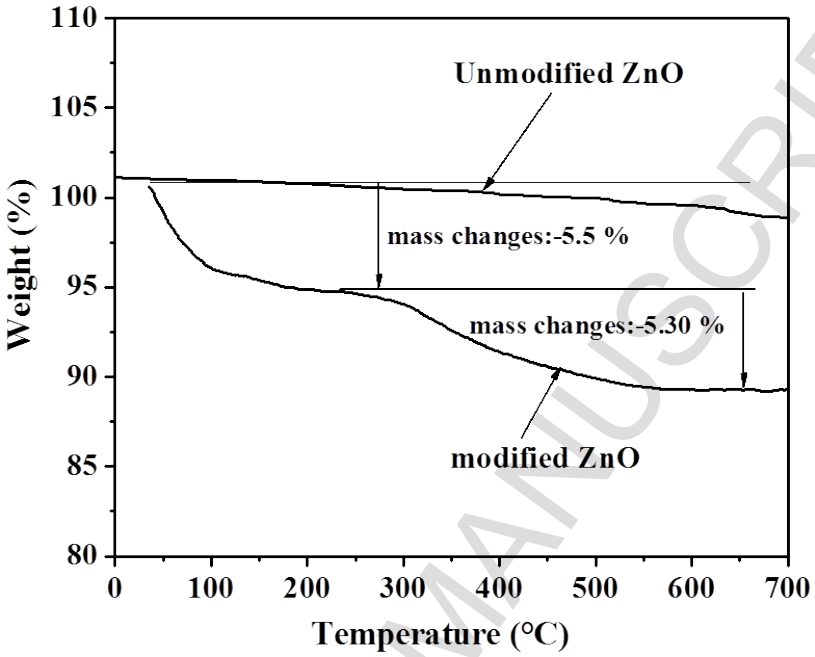

Fig. 4 TGA thermogram of unmodified ZnO nanoparticles (ZN) and PVA modified ZnO nanoparticles (PZN).

Typical XRD patterns of ZN and PZN are shown in Fig. 5 (a). Almost all the observed diffraction peaks of ZN and PZN can be indexed to wurtzite structure of ZnO (hexagonal phase, space group P63 mc, and JCPDS no. 36-1451). No new diffraction peak is observed in case of the PZN compared to that of the ZN. The crystallite size of unmodified and modified ZnO nanoparticles have been determined using Scherer's formula [39] and found as 43.5 and 32.7 nm. The XRD patterns show the capped polymer does not affect the crystallite structure of ZnO nanoparticles, which is found in close agreement with the results reported by others [40]. The average crystallite size of PZN is about 32.7 nm, which indicates that the capping agent plays a vital role in controlling the growth of the crystals during the synthesis process. Fig. 5(b) shows the EDX spectra of ZN and PZN, which indicates high level purity of nanoparticles. The presence of C atom in case of PZN shows an evidence of PVA bonding onto the surface of ZnO nanoparticles. The elemental analysis in atomic wt.% is depicted in Table 1. Thus, again it is verified that the surface of ZnO nanoparticles is successfully modified by the capping agent PVA.

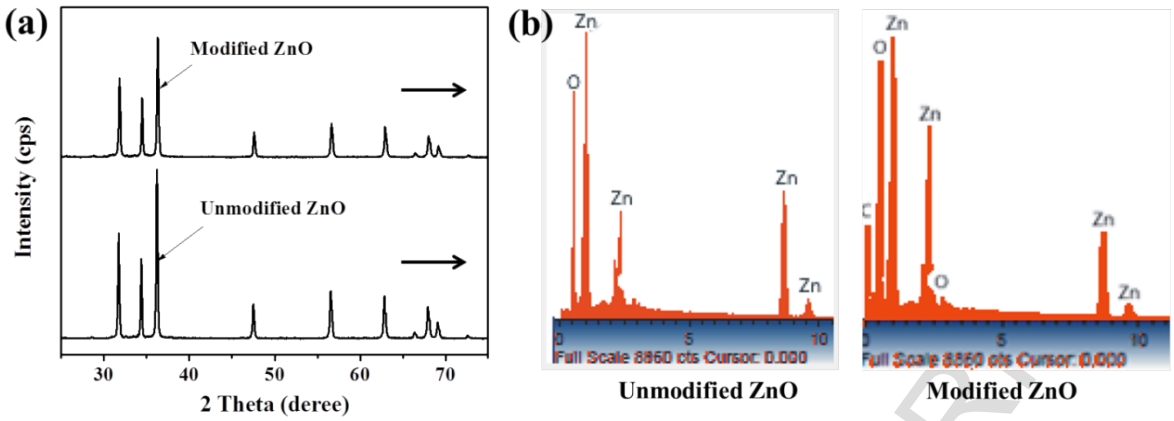

Fig. 5 (a) XRD pattern (b) EDX spectra of Unmodified ZnO nanoparticles (ZN) and PVA modified ZnO nanoparticles (PZN).

3.4. Dispersion behavior of nanocomposites

The FESEM micrographs of ZEC-1 and PZEC-1 are shown in Fig. 6. The image (Fig. 6 (a)) clearly indicates the particles in the agglomeration form, whereas the homogeneous distribution and dispersion of modified ZnO nanoparticles can be easily observed (Fig. 6 (b)) compared to that of the unmodified nanoparticles. The surface energy of the nanoparticles decreases due to the strong interaction between CH–OH groups of PVA and hydroxyl groups present on the surface of nanoparticles. The decrease in surface energy also reduces the clustering tendency of nanoparticles [41]. The curing behavior and the possible reaction mechanism of PVA modified ZnO nanoparticles with epoxy network are illustrated in Scheme-2. The possible interactions between the modified ZnO nanoparticles and epoxide groups have been shown through strong hydrogen bonding.

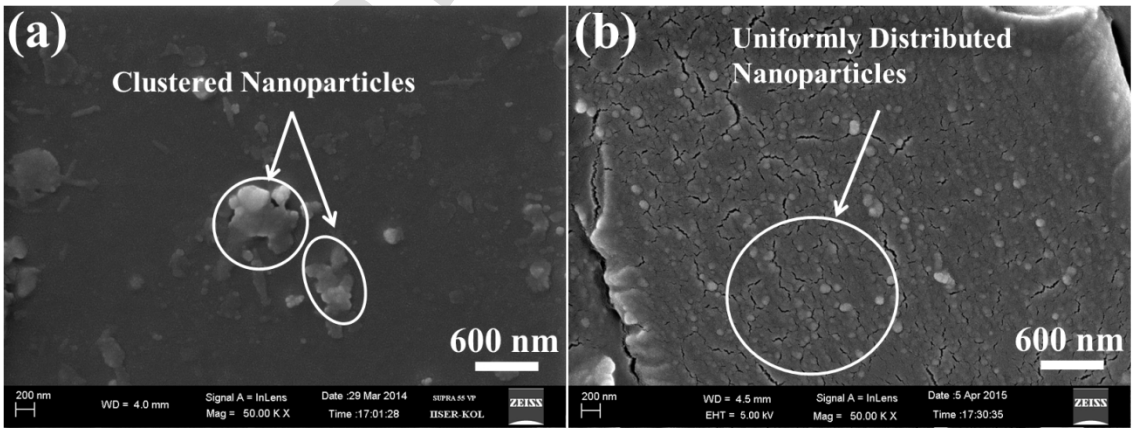

Fig. 6 FESEM micrographs of epoxy nanocomposites containing (a) unmodified ZnO nanoparticles (1 wt. %), (b) PVA modified ZnO nanoparticles (1 wt. %).

The polymer stabilizing agent, PVA also creates steric hindrance between inorganic nanoparticles to reduce their agglomeration [42].

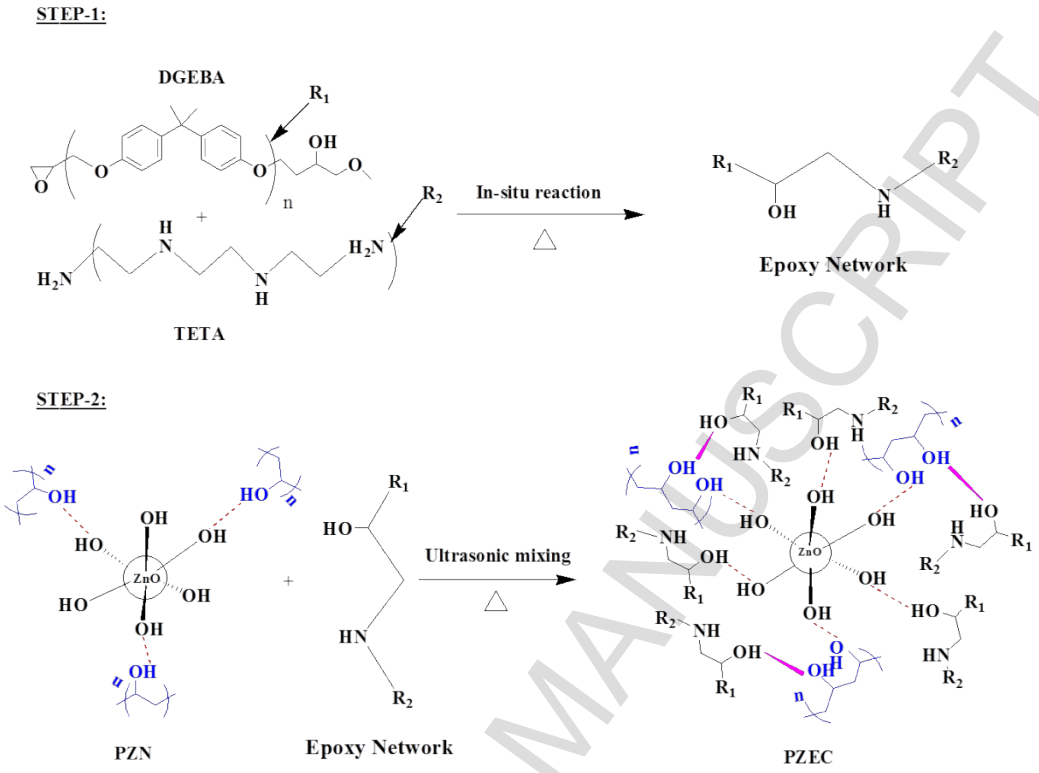

Scheme 2: Schematic representation of cuing reaction of epoxy network in presence of PZN.

3.5. Glass transition temperature and thermal stability of nanocomposites

The variation in glass transition temperature (T_g) versus the concentration of ZN and PZN in epoxy matrix is shown in Fig. 7. The increase in concentration of unmodified and modified nanoparticles upto 2 wt.% increases the T_g value of the composites. But, further increase in concentration from 2 to 3 wt.% results in decline in T_g value in both the cases. In case of modified nanoparticles reinforced epoxy matrix, the T_g value for each variation of nanoparticle content from 0 to 3 wt.%, is found higher than the unmodified particles reinforced epoxy. The maximum enhancement in T_g value of PZEC-2 is ~24% higher than the neat epoxy. This indicates the restriction offered by nanoparticles to the mobility of polymer chains of epoxy network [43-44]. Therefore, this enhancement in T_g value suggests strong interfacial interactions between the polymer matrix and surface modified ZnO nanoparticles through strong hydrogen bonding. The difference in T_g values may be due to the difference in the degree of cross-linking density of epoxy network. The higher value of T_g may be attributed to the higher degree of cross-linking density,

whereas low value of T_g with increase in particle content may be attributed to the non-homogeneous dispersion of nanoparticles in the epoxy network [45-46].

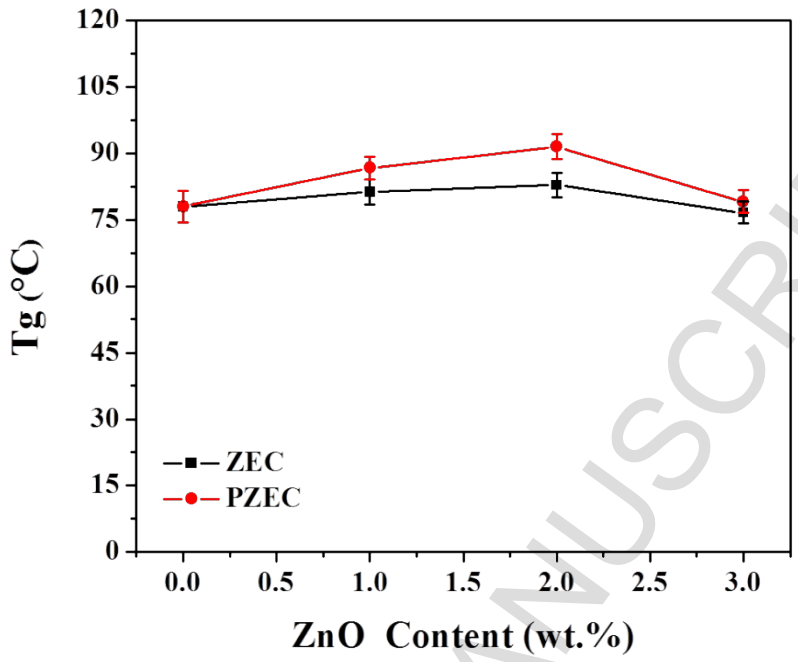

Fig. 7 Variation in glass transition temperature (T_g) with respect to concentration of ZN and PZN in epoxy matrix.

The TGA curves of unmodified and modified epoxy nanocomposites containing 1-3 wt.% of ZnO are shown in Fig. 8. The TGA plots clearly reveal single step degradation behavior for each concentration of unmodified and modified nanocomposites. The value of T_{IDT} (initial decomposition temperature, 5% wt. loss), T_{MDT} (maximum decomposition temperature, 50% wt. loss) and char yield percentage (CYP) of the composites measured from TGA plots are illustrated in Table. 2.

Table. 2 Thermal properties of NE, PVA modified and unmodified ZnO/epoxy nanocomposites.

Samples	ZnO content (wt. %)	T_{IDT} (°C)	T_{MDT} (°C)	Char yield (%) at (700°C)
NE	0	310.5	375	10.91
Modified ZnO/epoxy nanocomposites				
PZEC-1	1	319.6	376.5	15.04
PZEC-2	2	326.3	381.5	17.52
PZEC-3	3	322.9	377.8	14.37
Unmodified ZnO/epoxy nanocomposites				
ZEC-1	1	324.7	375.5	11.47
ZEC-2	2	319.8	376.5	12.68
ZEC-3	3	300	373.7	10.69

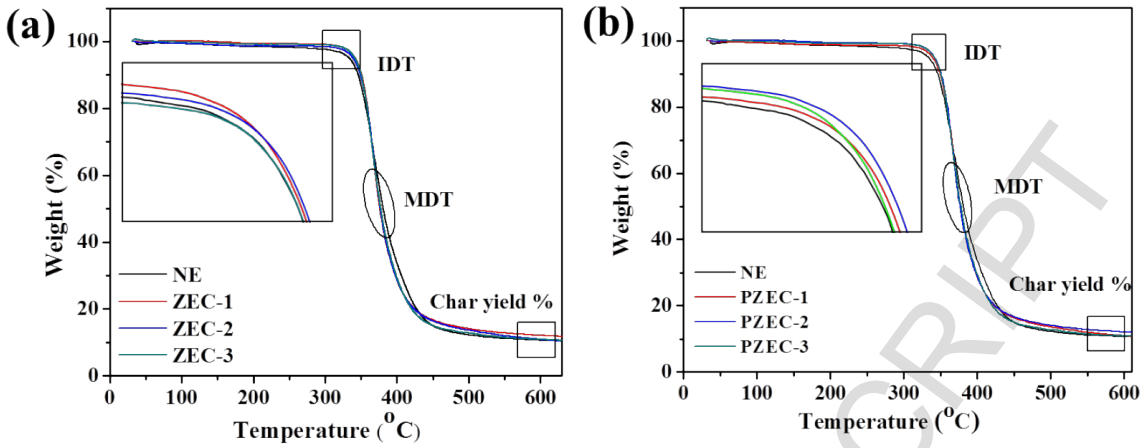

Fig. 8 TGA curve of (a) unmodified ZnO epoxy nanocomposites (b) PVA modified ZnO epoxy nanocomposites.

Fig. 8 shows the addition of both unmodified and modified nanoparticles in epoxy network results in improved thermal resistance of the composite. It was observed that the decomposition temperature of PZEC-2 slightly improves the T_{IDT} (326.3 ºC) by 16 ºC with respect to NE (310.5 ºC). Similar trend was also observed in case of ZEC-3, but comparatively less enhancement in T_{IDT} by 10 ºC with respect to NE. Moreover, the increase in T_{IDT} is an indicative of the homogeneous dispersion of ZnO in epoxy matrix which acts as obstacles to heat flow through the matrix [11, 47-49]. The char yield percentage (CYP) of unmodified and modified nanocomposites increases with the increase in particle content. It is obvious that the thermal degradation of inorganic nanoparticles is higher as compared to the polymer matrix. Therefore, due to addition of nanoparticles in the matrix, the overall thermal stability of nanocomposites increases. Moreover, these modified and unmodified ZnO nanoparticles forms residue in nitrogen atmosphere. Maximum CYP of PZEC-2 compared to other composites demonstrates its potential to hinder the decomposition at high temperature. Thus, it infers that the PVA modified ZnO nanoparticles have the potential to restrict the thermal decomposition of the epoxy network, which may be due to their nanorod like morphology with high aspect ratio compared to the unmodified nanoparticles.

3.6. Mechanical properties

3.6.1. Tensile and compressive properties

Fig. 9 shows the tensile and compressive properties of unmodified and modified ZnO nanoparticles reinforced epoxy composites. The tensile strength, tensile modulus and compressive strength was found increased with the increase in filler content up to 2 wt.% but decreased with the further increase in ZnO content. The measured values

of tensile strength, tensile modulus and compressive strength for NE are 55 MPa, 2.85 GPa and 120 MPa, respectively. The maximum enhancements in tensile strength, modulus and compressive strength of PZEC-2 compared to the neat epoxy system are ~24%, ~47% and ~48%, respectively. Furthermore, the decrease in tensile strength, tensile modulus and compressive strength at higher nanoparticle content may be attributed to the agglomeration of nanoparticles in matrix due to high surface energy and large surface area of the ZnO nanoparticles.

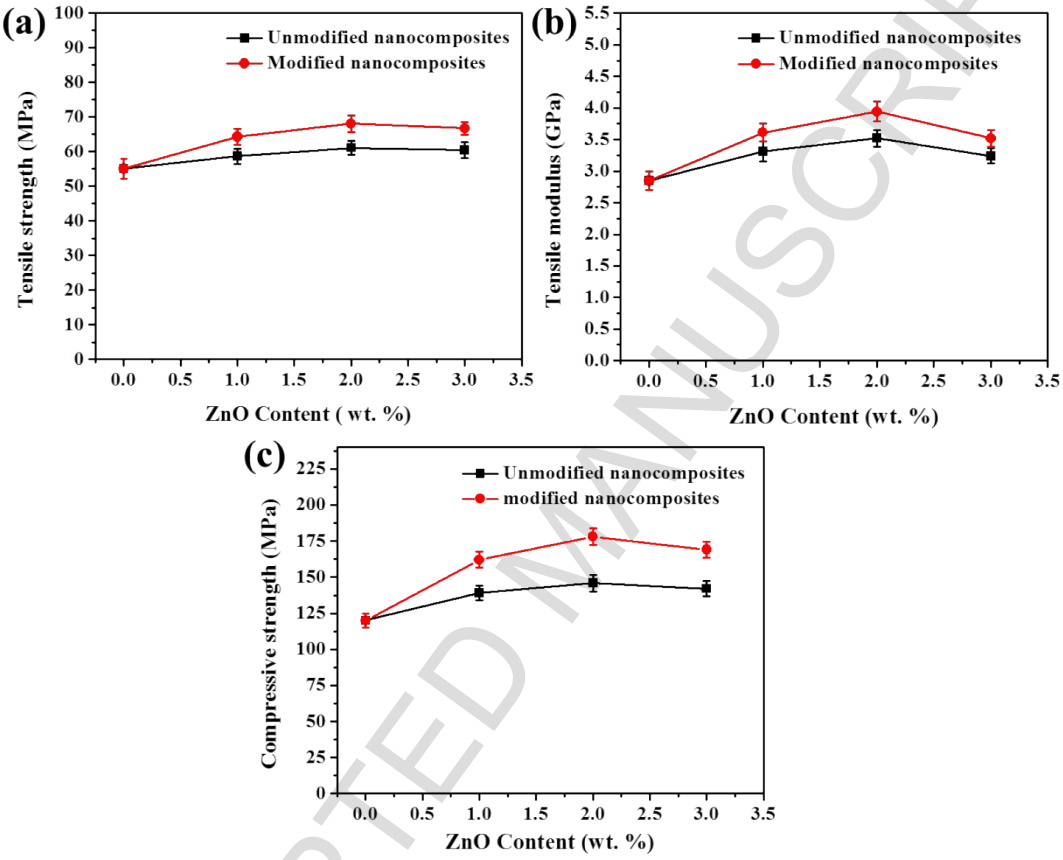

Fig. 9 Tensile and compressive properties of epoxy nanocomposites: variation in (a) tensile strength (b) tensile modulus and (c) compressive strength; with respect to the concentration of ZN and PZN.

The above hypothesis is supported by the FESEM images of the nanocomposites at higher filler contents (3 wt.%). A microscopic image of epoxy nanocomposites reinforced with modified ZnO at particles content 1, 2 and 3 wt.% is shown in Fig. 10 (a-c). From Fig. 10 (b), it is clear that maximum distribution of particles into the matrix is achieved with 2 wt.% loading while at 3 wt.% ZnO nanoparticles tend to aggregate as shown in Fig. 10 (c).

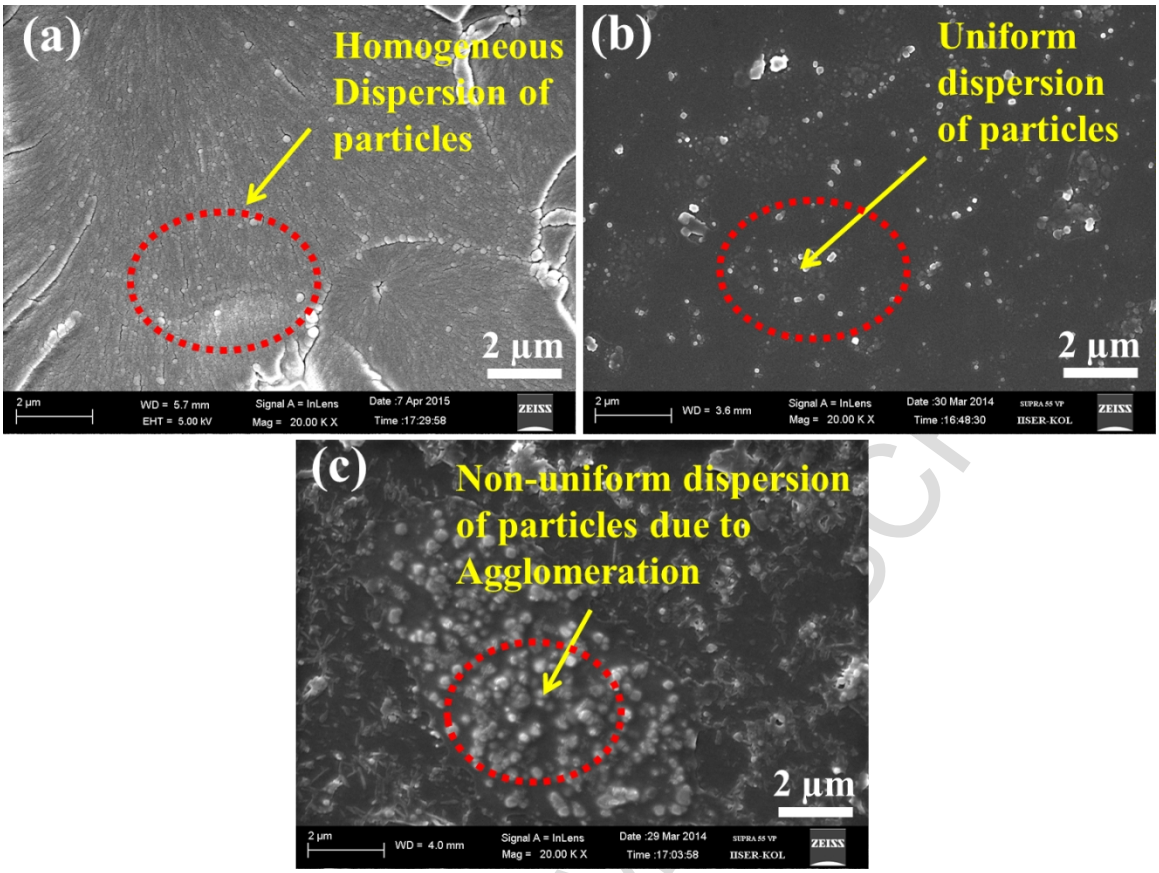

Fig. 10 FESEM images of epoxy nanocomposites containing (a) 1 wt. % PZN, (b) 2 wt. % PZN, (c) 3 wt. % PZN.

It is fact that the reinforcing capability of PZN in epoxy resin system was better than that of ZN. The mechanical properties of the epoxy nanocomposites strongly depend on the proper dispersion of fillers in the polymer matrix along with a good interaction between them. After grafting of ZnO with PVA, the surface energy gets reduced resulting in effective dispersion and strong adhesion at the interface and thereby improving tensile properties of nanocomposites. So, in comparison to unmodified ZnO nanoparticles, the modified ZnO nanoparticles show superior mechanical properties may be due to strong chemical bond formation between modified nanoparticles and the epoxy matrix. It is suggested that the use of PVA modified ZnO nanoparticles in composites can significantly improve effective dispersion and compatibility with polymer matrix.

3.6.2. Flexural property

Fig. 11 shows the flexural properties of unmodified and modified nanoparticle reinforced epoxy composites. The flexural strength and modulus of unmodified and modified ZnO/epoxy nanocomposites increase with the increase in particle content up to 2 wt.% and then decline with the further increase in particle content from 2 to 3 wt.%.

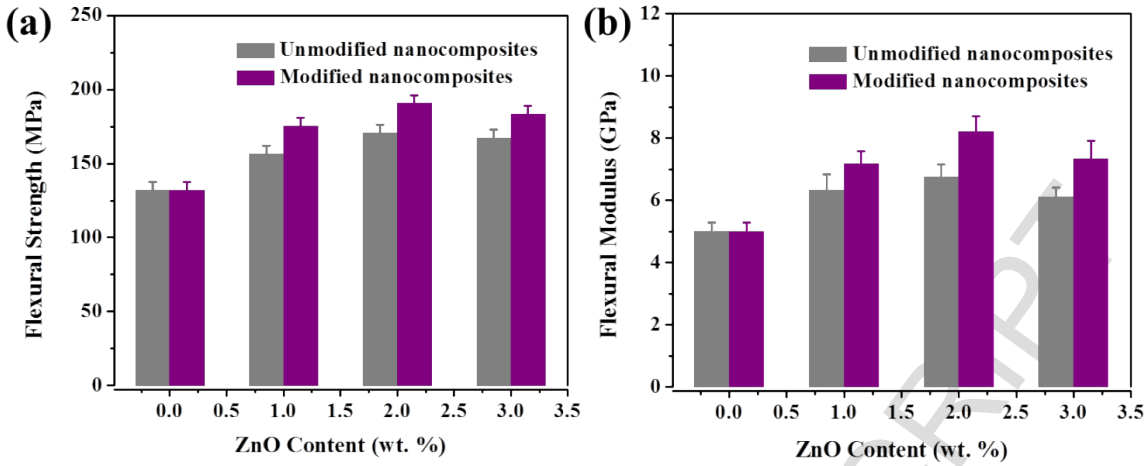

Fig. 11 Flexural properties of epoxy nanocomposites: Variation in (a) flexural strength and (b) flexural modulus; with respect to the concentration of ZN and PZN.

The maximum enhancement in flexural strength and modulus of PZEC-2 compared to the neat epoxy system are ~44% and ~64% respectively. In comparison to unmodified ZnO nanoparticles, the modified ZnO nanoparticles show better flexural properties that may be due to the formation of strong chemical bond at interface between the modified ZnO nanoparticles and epoxy network. Similar results were also reported in the case of other nanofillers based nanocomposites [50]. Thus, it can be inferred that the surface modification of ZnO nanoparticles leads to the significant improvement in mechanical properties of the epoxy nanocomposites.

3.6.3. Fracture toughness and fracture energy

The effect of unmodified and modified ZnO nanoparticles content on fracture toughness (K_{Ic}) and fracture energy (G_{Ic}) of nanocomposites is shown in Fig. 12, where error bars indicate the maximum and minimum values. The K_{Ic} and G_{Ic} values of NE are ~0.46 MPa.m$^{1/2}$ and 37.42 J/m^2 respectively. The addition of 2 wt.% of modified ZnO particles into the epoxy matrix results an increase in K_{Ic} value of ~0.79 MPa.m$^{1/2}$, which corresponds to ~49% increase in the fracture toughness. For higher nanoparticle content (3 wt.%), the K_{Ic} reduces to ~0.69 MPa.m$^{1/2}$, which is found still higher than that of the neat epoxy matrix. Similar trend of K_{Ic} value is observed in case of ZEC and PZEC nanocomposites at 2 wt.% filler concentration. To achieve same enhancement (~49%) in K_{Ic}, the required amount of (wt.%) titania, alumina and silica nanoparticles in epoxy matrix is quite high [51-53]. This reflects the potential of low content of modified ZnO nanoparticles to reinforce the epoxy matrix.

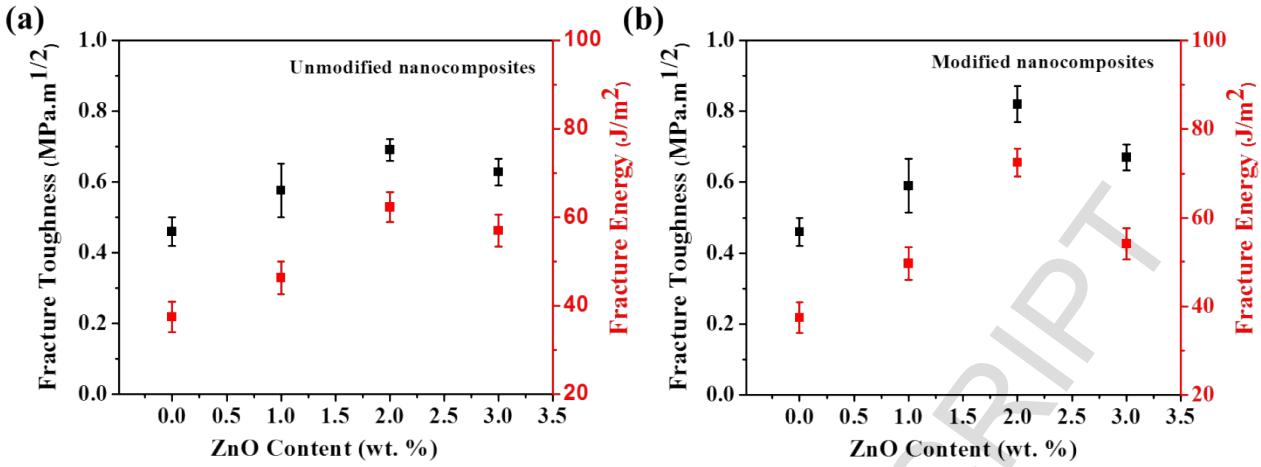

Fig. 12 Fracture toughness of epoxy nanocomposites: Variation of fracture toughness (K_{Ic}) and fracture energy (G_{Ic}) as a function of (a) unmodified and (b) modified ZnO nanoparticle content in epoxy matrix.

The fracture energy of the epoxy nanocomposites have been calculated using the relation: $G_{Ic} = K^2_{Ic}\,[(1-\mu^2)/E]$, where μ is Poisson's ratio [54]. The fracture energy (G_{Ic}) enumerates the energy required for crack propagation in a material. The calculated G_{Ic} of NE is 280 J/m^2. At 2 wt.% loading of PZEC (PZEC-2), the composite shows ~95% enhancement in G_{Ic} (545 J/m^2) with respect to that of NE. However, further increase in nanoparticle content up to 3 wt.% (i.e., PZEC-3) leads to a reduction in the fracture energy of the composite. This noticeable enhancement in energy release rate of the nanocomposite is comparable to tough polymers reinforced with other organic or inorganic nanofillers [55]. These results exhibit the potential of low content of modified ZnO nanofiller in toughening the epoxy polymer. All mechanical properties such as tensile strength, compressive strength, elastic modulus, flexural strength, flexural modulus, fracture toughness and fracture energy show a consistent improvement with increase in modified ZnO nanofillers content up to 2 wt.% and on further addition of filler, efficiency gets reduced. This is happening due to clustering of ZnO nanoparticles which aids to diminish the interfacial contact area at ZnO/epoxy matrix interface and hence, it weakens the ability of the ZnO to reinforce the composite. The clustering leads to poor interaction between the nanofiller and epoxy matrix because; the clusters act as defect centers in the epoxy matrix causing a detrimental effect on the mechanical properties.

3.7 Microscopic investigation of fracture surfaces

FESEM images of tensile fracture surface of NE, epoxy nanocomposites containing 2 and 3 wt.% of unmodified and modified ZnO particle content are shown in Fig. 13 (a-e). The fracture surface of NE (Fig. 13a) shows relatively

smooth and glassy texture, which suggests poor absorption of energy during crack propagation resulting in brittle fracture. However, the fracture surface of epoxy nanocomposites containing unmodified ZnO nanoparticles such as ZEC-2 and ZEC-3 (Fig. 13(b, d)) shows less rough surface compared to that of epoxy nanocomposites (PZEC-2 and PZEC-3) containing modified ZnO nanoparticles (Fig. 13(c, e))..

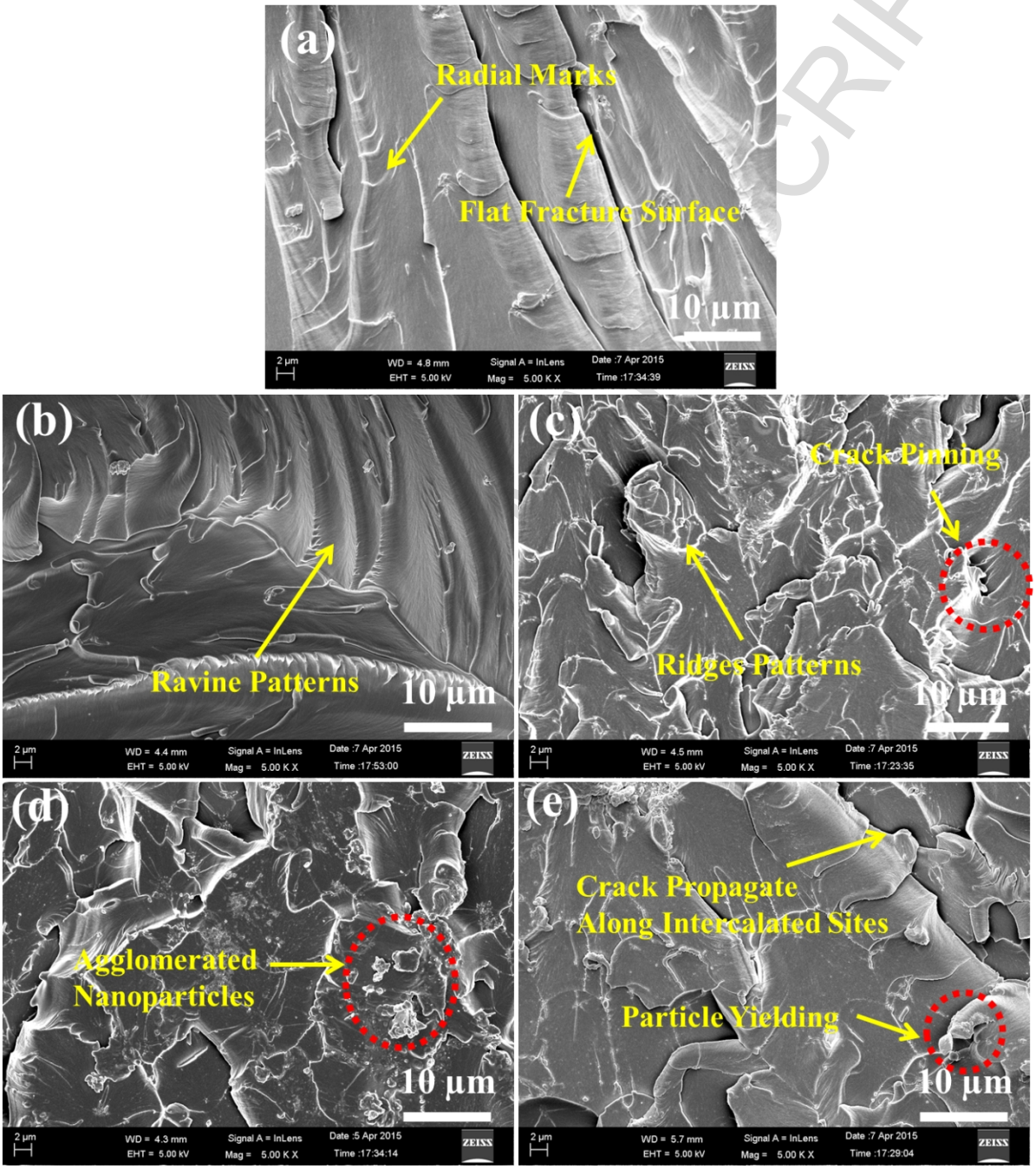

Fig. 13 Tensile fracture surfaces of (a) NE (b) ZEC-2 (c) PZEC-2 (d) ZEC-3 and (e) PZEC-3.

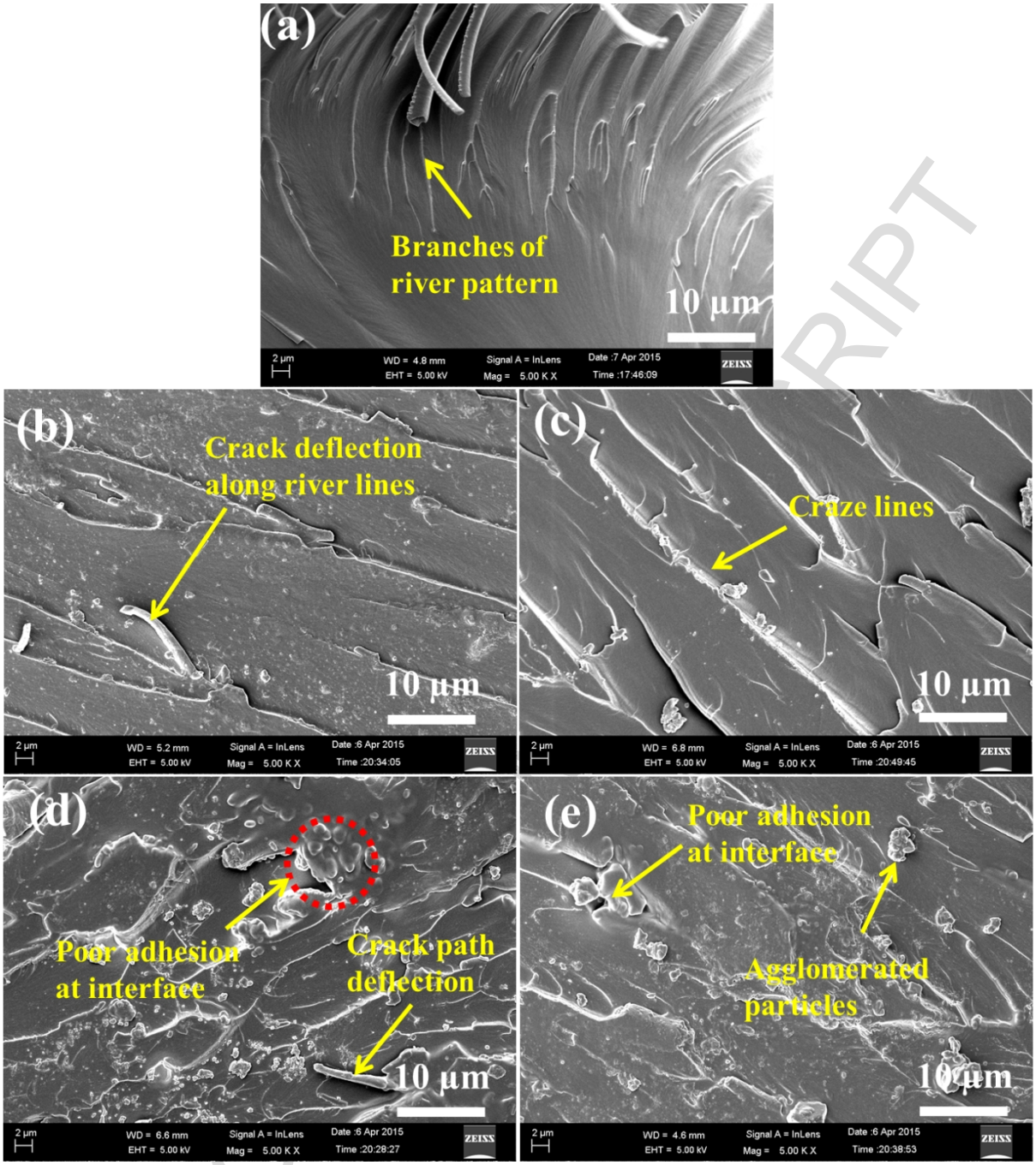

Fig. 14 FESEM micrographs showing the failure mechanisms of the fracture surface obtained from the 3-point bending specimens of (a) NE (b) ZEC-2 (c) PZEC-2 (d) ZEC-3 and (e) PZEC-3.

The fracture surface of the epoxy nanocomposite containing unmodified ZnO nanoparticles shows ravine patterns like texture and the surfaces between the ravine patterns is relatively smooth, which are the characteristic features of brittle fracture behaviour. However, the fracture surfaces of epoxy nanocomposites containing modified ZnO

nanoparticles shows substantial increase in the surface roughness due to the presence of large number of dimples and ridges, which is a measure of enhanced restriction to crack propagation and thus enhanced the toughness of material. The modified ZnO nanoparticles reinforced in highly cross linked polymer network diverts the crack path in different direction thereby delaying the crack propagation and absorbing more energy prior to failure. As a result of crack divergence in random directions, crack pinning and shear yielding zones were observed on the fracture surface which may be attributed to increase in overall tensile strength and stiffness of the nanocomposites [56]. FESEM images of SENB fracture surface of NE, epoxy nanocomposites containing 2 and 3 wt.% of unmodified and modified ZnO particle content are shown in Fig. 14 (a-e). The fracture surface of NE (Fig. 14a) shows the smooth surface with branches of river pattern depicting brittle failure. However, the introduction of ZnO nanoparticles into the epoxy network shows localized shear yielding zones like shear bands, river lines and crazing lines (Fig. 14 (b-e)). These zones may restrict the crack propagation resulting in absorption of more energy prior to failure of the material. But, the craze line features observed on the fracture surfaces of epoxy nanocomposites containing modified ZnO nanoparticles may absorb more energy and result in slow crack propagation and develop more number of shiny river lines and shear yielding zone. Moreover, the appearance of increased number of river lines increases the surface roughness justifying the enhanced fracture toughness of PZEC (Fig. 14 (c, e)) as compared to the ZEC (Fig. 14 (b, d))

Conclusion

Poly vinyl alcohol (PVA)-assisted ZnO nanoparticles with nanorod like morphology was successfully synthesized using sol-gel technique. Better dispersion of 2 wt.% modified ZnO nanoparticles in epoxy polymer was achieved compared to the same concentration of unmodified particles. A lower concentration (~2 wt.%) of unmodified and modified ZnO nanoparticles for obtaining improved thermal and mechanical properties of the epoxy composites was identified. A significant improvement in T_g and minor improvement in thermal stability were achieved for synthesized epoxy nanocomposites. The improvement in modified ZnO nanoparticles reinforced composite was superior to unmodified particle reinforced epoxy composite at same nanofiller content (2 wt.%). The mechanical properties including the tensile strength, tensile modulus, compressive strength, flexural strength and flexural modulus were significantly increased in case of modified ZnO nanoparticles reinforced composite at 2 wt.% nanoparticle concentration. The reduced thermal and mechanical properties of epoxy nanocomposites for higher

concentration of nanoparticles might be due to non-homogeneous particle dispersion in the highly viscous epoxy resin system. The tensile and SENB test fracture surfaces of unmodified and modified ZnO/epoxy nanocomposites showed the various toughening mechanisms like branching of river lines, regular river lines and craze lines. The improved roughness of fracture surface of ZnO nanoparticles reinforced composites significantly improved the fracture toughness. These results show the potential of surface modified ZnO nanoparticles to enhance the thermal and mechanical properties of epoxy nanocomposites.

Acknowledgement

This work was supported by start-up research grant from National Institute of Technology Silchar with Grant No. Dean (RC)/457/122. Authors are also thankful to Department of Science and Technology, India to provide support under DST-FIST programme 2014 with Grant No. SR/FST/ ETI-373/2014.

References

[1] C. Velasco-Santos, A.L. Martínez-Hernández, F.T. Fisher, R.S. Ruoff, V.M. Castaño Improvement of Thermal and Mechanical Properties of Carbon Nanotube Composites through Chemical Functionalization, Chem. Mater. 15 (2003) 4470–4475.

[2] S. Bal, Experimental study of mechanical and electrical properties of cnf/epoxy composites, Mater. Des. 31 (2010) 2406–2413.

[3] S. Halder. P.K Ghosh, A. Pathak, M.S Goyat, Influence of nanoparticle weight fraction on morphology and thermal properties of epoxy/TiO2 nanocomposite, J. Reinf. Plast. Compos. 31 (2012) 1180–1188.

[4] S. Halder, M.S. Goyat, P.K. Ghosh, Influence of ultrasonic dual mode mixing on morphology and mechanical properties of ZrO2-epoxy nanocomposite, High Perform. Polym. 24 (2012) 331–341.

[5] A. Jumahat, C. Soutis, S.A. Abdullah, S. Kasolang, Tensile properties of nanosilica/epoxy nanocomposites, Procedia Eng. 41 (2012) 1634–1640.

[6] J. Cho, M.S. Joshi, C.T. Sun, Effect of inclusion size on mechanical properties of polymeric composites with micro and nano particles, Compos. Sci. Technol. 66 (2006) 1941–1952.

[7] C. Xu, P. Shin, L. Cao, D. Gao, Preferential Growth of Long ZnO Nanowire Array and Its Application in Dye-Sensitized solar cells, J. Phys. Chem. C. 114 (2010) 125–129.

[8] A. Z. Sadek, S. Choopun, W. Wlodarski, S.J. Ippolito, K.K. Zadeh, Characterization of ZnO Nanobelt-Based Gas Sensor for H_2, NO_2, and Hydrocarbon Sensing, IEEE Sens. J. 7 (2007) 919–924.

[9] T. Goto, S. Yin, T. Sato, T. Tanaka, Morphological Control of Zinc Oxide and Application to Cosmetics, Int. J. Nanotechnol. 10 (2013) 1–4.

[10] A.M. Díez-Pascual, A.L. Díez-Vicente, High-performance aminated poly(phenylene sulfide)/ZnO nanocomposites for medical applications, ACS Appl. Mater. Interfaces. 6 (2014) 10132–10145.

[11] T. Prasad, S. Halder, M.S. Goyat, S.S. dhar, Morphological Dissimilarities of ZnO Nanoparticles and its effect on Thermo-Physical Behavior of Epoxy composites, Polym. Compos. (2016) 1–11.

[12] T. Prasad, S. Halder, Optimization of Parameters and its Effect on Size of ZnO Nanoparticles Synthesized by Sol-gel Method, Comput. Probl. Solving, Adv. Intelligient Syst. Comput. 336 (2015) 403–411.

[13] G.J. Ehlert, H.A. Sodano, Zinc Oxide Nanowire Interphase for enhenced strength in lightweight polymer fiber composites, Appl. Mater. INTERFACES. 1 (2009) 1827–1833.

[14] S. Halder, S. Ahemad, S. Das, J. Wang, Epoxy/Glass Fiber Laminated Composites Integrated with Amino Functionalized ZrO2 for Advanced Structural Applications, ACS Appl. Mater. Interfaces. 8 (2016) 1695–1706.

[15] M. Murariu, A. Doumbia, L. Bonnaud, A.L. Dechief, Y. Paint, M. Ferreira, C. Campagne, E. Devaux, P. Dubois, High-performance polylactide/ZnO nanocomposites designed for films and fibers with special end-use properties, Biomacromolecules. 12 (2011) 1762–1771.

[16] M. Z. Rong, M.Q. Zhang, W.H. Ruan, Surface modification of nanoscale fillers for improving properties of polymer nanocomposites: a review, Mater. Sci. Technol. 22 (2006) 787–796.

[17] H. baier Zhi-Quiang Yu, Shu-Li You, Effect of Organosilane Coupling Agents on Microstructure and Properties of Nanosilica/epoxy Composites, Polym. Compos. (2012) 1516–1524.

[18] J. Kathi, K.Y Rhee, J.H. Lee, Effect of chemical functionalization of multi-walled carbon nanotubes with 3-APTES on mechanical and morphological properties of epoxy nanocomposites, Compos. Part A. 40 (2009) 800–809.

[19] S. Mallakpour, M. Dinari, E. Azadi, Poly (vinyl alcohol) Chains Grafted onto the Surface of Copper Oxide Nanoparticles : Application in Synthesis and Characterization of Novel Optically Active and Thermally Stable Nanocomposites Based on Poly (amide-imide) Containing N - trimellitylimid, Int. J. Polym. Anal. Charact. 20 (2015) 1–16.

[20] S. Kayal, R. V. Ramanujan, Doxorubicin loaded PVA coated iron oxide nanoparticles for targeted drug delivery, Mater. Sci. Eng. C. 30 (2010) 484–490.

[21] M. Z. Rong, M. Q. Zhang, W. H. Ruan, Surface modification of nanoscale fillers for improving properties of polymer nanocomposites: a review. Materials Science and Technology 22 (2006) 787-796.

[22] K.H. Ding, G.L. Wang, M. Zhang, Characterization of mechanical properties of epoxy resin

reinforced with submicron-sized ZnO prepared via in situ synthesis method. Materials and Design 32 (2011) 3986–3991.

[23] R. D. Rashmi, T.K. Maji, Effect of Nano-ZnO on Thermal, Mechanical, UV Stability, and Other Physical Properties of Wood Polymer Composites. Ind. Eng. Chem. Res. 51 (2012) 3870−3880.

[24] S. Mallakpour, M. Javadpour, Effective Methodology for the production of Novel Nanocomposites Films based on Poly(vinyl chloride) and Zinc Oxide Nanoparticles Modified With Green PVA, Polym. Compos. (2015) 1–10.

[25] X.L Xiea, R.K.Y. Lic, Q.X Liua, Y.W. Mai, Structure-property relationships of in-situ PMMA modified nano-sized antimony tri-oxide filled PVC nanocomposites, Polymer. 45 (2004) 2793–2802.

[26] A. Chatterjee, S. Mishra, Rheological, Thermal and Mechanical Properties of Nano-Calcium Carbonate (CaCO3)/PMMA Core-Shell Nanoparticles Reinforced Polypropylene Composites, Polym. Soc. Korea. (2012) 1–10.

[27] W. Yang, R. Yi, Xu Yang, M. Xu, S. Hui, X. Cao, Effect of Particle Size and Dispersion on Dielectric Properties in ZnO/Epoxy Resin Composites. Trans. Electr. Electron. Mater. 13(3) 116 (2012).

[28] B. Ramezanzadeh, M.M. Attar. M. Farzam, Effect of ZnO nanoparticles on the thermal and mechanical properties of epoxy-based nanocomposite. J Therm Anal Calorim 103 (2011) 731–739.

[29] D.Q. H. Zhang, D. Yang, D. Li, X. Ma, Controllable Growth of ZnO Microcrystals by a capping-molecules-Assisted Hydrothermal Process, Cryst. Growth Des. 5 (2005) 547–550.

[30] K. Biswas, B. Das, C.N.R. Rao, Growth Kinetics of ZnO Nanorods- Capping-Dependent Mechanism and Other Interesting, J. Phys. Chem. C. 112 (2008) 2404–2411.

[31] K. Yong, Youngio Tak, Controlled Growth of Well-Aligned ZnO Nanorod Array Using a Novel Solution Method, J. Phys. Chem. C. 109 (2005) 19263–19269.

[32] N.R. Yogamalar, R. Srinivasan, A.C. Bose, Multi-capping agents in size confinement of ZnO nanostructured particles, Opt. Mater. (Amst). 31 (2009) 1570–1574.

[33] S. Simon P. Garcia, Controlling the Morphology of Zinc Oxide Nanorods Crystallized from the Aqueous Solutions: The Effect of Crystal Growth Modifiers on Aspect Ratio, Chem. Mater. 19 (2007) 4016–4022.

[34] R. Viswanatha, D.D. Sharma, Study of the Growth of Capped ZnO Nanocrystals:A Rout to Rational Synthesis, Chem Eur. J. 12 (2006) 180–186.

[35] C.C. Vidyasagar, Y. Arthoba Naik, Surfactant (PEG 400) effects on crystallinity of ZnO nanoparticles, Arab. J. Chem. 9 (2016) 507–510.

[36] L. Kumari, W.Z. Li, S. Kulkarni, K.H. Wu, W. Chen, C. Wang, C.H. Vannoy, R.M. Leblanc, Effect

of Surfactants on the Structure and Morphology of Magnesium Borate Hydroxide Nanowhiskers Synthesized by Hydrothermal Route, Nanoscale Res. Lett. 5 (2010) 149–157.

[37] C. Dinh, T. Nguyen, F. Kleitz, T. Do, Shape-Controlled Synthesis of Highly Crystalline Titenia Nanoparticles, ACS Nano. 3 (2009) 3737–3743.

[38] K. Akhil, J. Jayakumar, G. Gayathri, S.S. Khan, Effect of various capping agents on photocatalytic, antibacterial and antibiofilm activity of ZnO nanoparticles, J. Photochem. Photobiol. BBiology. 160 (2016) 32–42.

[39] A.K. Srivastava, M. Deepa, N. Bahadur, M.S. Goyat, Influence of Fe doping on nanostructures and photoluminescence of sol-gel derived ZnO, Mater. Chem. Phys. 114 (2009) 194–198.

[40] A.N. Mallika, A.R. Reddy, K.V. Reddy, Annealing effects on structural and optical properties of ZnO nanoparticles with PVA and CA as chelating agent, J. Adv. Ceram. 4 (2015) 123–129.

[41] R.K. S. Kango, S. kalia, A. celli, J. Njuuna, Y. Habbibi, Surface modification of inorganic nanoparticles for development of organic-inorganic nanocomposites-A Review, Prog. Polym. Sci. 38 (2013) 1232–1261.

[42] S. Mallakpour, M. Dinari, M. Hatami, Dispersion of surface-modified nano-Fe3O4 with poly(vinyl alcohol) in chiral poly(amide-imide) bearing pyromellitoyl-bis-l-phenylalanine segments, J. Mater. Sci. 50 (2015) 2759–2767.

[43] P. Li, X. Chen, J.-B. Zeng, L. Gan, M. Wang, Enhancement of the interfacial interaction between poly(vinyl chloride) and zinc oxide modified reduced graphene oxide, RSC Adv. 6 (2016) 5784–5791.

[44] B. Ramezanzadeh, M.M. Attar, M. Farzam, Effect of ZnO nanoparticles on the thermal and mechanical properties of epoxy-based nanocomposite, J. Therm. Anal. Calorim. 103 (2011) 731–739.

[45] K.W. Putz, M.J. Palmeri, R.B. Cohn, R. Andrews, L.C. Brinson, Effect of Cross-Link Density on Interphase Creation in Polymer Nanocomposites, Macromolecules. 41 (2008) 6752–6756.

[46] V.I. Roldughin, O.A. Serenko, E. V Getmanova, N.A. Novozhilova, G.G. Nikifirova, M.I. Buzin, S.N. Chvalun, A.N. Ozerin, A.M. Muzafarov, Effect of Hybrid Nanoparticles on Glass Transition Temperature of Polymer Nanocomposites, Polym. Compos. (2016).

[47] B. Natarajan, Y. Li, H. Deng, L.C. Brinson, Linda S. Schadler, Effect of Interfacial Energetics on Dispersion and Glass Transition Temperature in Polymer Nanocomposites. Macromolecules 46 (2013) 2833−2841.

[48] S. Chandran, J.K. Basu, Effect of nanoparticle dispersion on glass transition in thin films of polymer nanocomposites. Eur. Phys. J. E 34 (2011) 1-5.

[49] Y. Sun, Z. Zhang, K.S Moon, C. P. Wong, Glass Transition And Relaxation Behavior Of Epoxy

Nanocomposites. Journal Of Polymer Science: Part B: Polymer Physics, 42 (2004) 3849–3858.

[50] Y. Zhou, L. Li, Y. Chen, H. Zou, M. Liang, Enhanced mechanical properties of epoxy nanocomposites based on graphite oxide with amine-rich surface, RSC Adv. 5 (2015) 98472–98481.

[51] H. Zhang, Z. Zhang, K. Friedrich, C. Eger, Property improvements of in situ epoxy nanocomposites with reduced interparticle distance at high nanosilica content, Acta Mater. 54 (2006) 1833–1842.

[52] H. baier Zhi-Quiang Yu, Shu-Li You, Effect of Surface Functional Modification of Nano Alumina Particles on Thermal and Mechanical Properties of Epoxy Nanocomposites, Adv. Compos. Mater. 20 (2011) 487–502.

[53] K. Kumar, P.K. Ghosh, A. Kumar, Improving mechanical and thermal properties of TiO2-epoxy nanocomposite, Compos. Part B Eng. 97 (2016) 353–360.

[54] K. Wang, J. Wu, L. Chen, C. He, M. Toh, Epoxy Nanocomposites With Highly Exfoliated Pristine Clay:Mechanical Properties and Fracture mechanisms, Macromolecules. 38 (2004) 1820–1824.

[55] N. Domun, H. Hadavinia, T. Zhang, T. Sainsbury, G.H. Liaghat, S. Vahid, Improving the fracture toughness and the strength of epoxy using nanomaterials – a review of the current status, Nanoscale. 7 (2015) 10294–10329.

[56] M.S. Goyat, A.S. Sumit, B. Sumit, S. Halder, P. Ghosh, Thermomechanical response and Toughening mechanisms of a carbon nano bead reinforced epoxy composite, Mater. Chem. Phys. 166 (2015) 144–152.

Captions:

Scheme. 1. Schematic representation of reaction mechanism between PVA monomer and hydroxyl groups of ZnO nanoparticles.

Fig. 1 Morphology of (a) unmodified ZnO nanoparticle (ZN) and (b) PVA modified ZnO nanoparticles (PZN).

Fig. 2 (a) Morphology of modified ZnO nanoparticle at high magnification (b) Histogram of particle size distribution of Unmodified ZnO nanoparticle (ZN) and PVA Modified ZnO nanoparticle (PZN).

Fig. 3 (a) FTIR spectra of Unmodified ZnO nanoparticle (ZN) and PVA modified ZnO nanoparticle (PZN).

Fig. 4 TGA thermogram of unmodified ZnO nanoparticles (ZN) and PVA modified ZnO nanoparticles (PZN).

Fig. 5 (a) XRD pattern (b) EDX spectra of Unmodified ZnO nanoparticles (ZN) and PVA modified ZnO nanoparticles (PZN).

Fig. 6 FESEM micrographs of epoxy nanocomposites containing (a) unmodified ZnO nanoparticles (1 wt. %), (b) PVA modified ZnO nanoparticles (1 wt. %).

Tables:

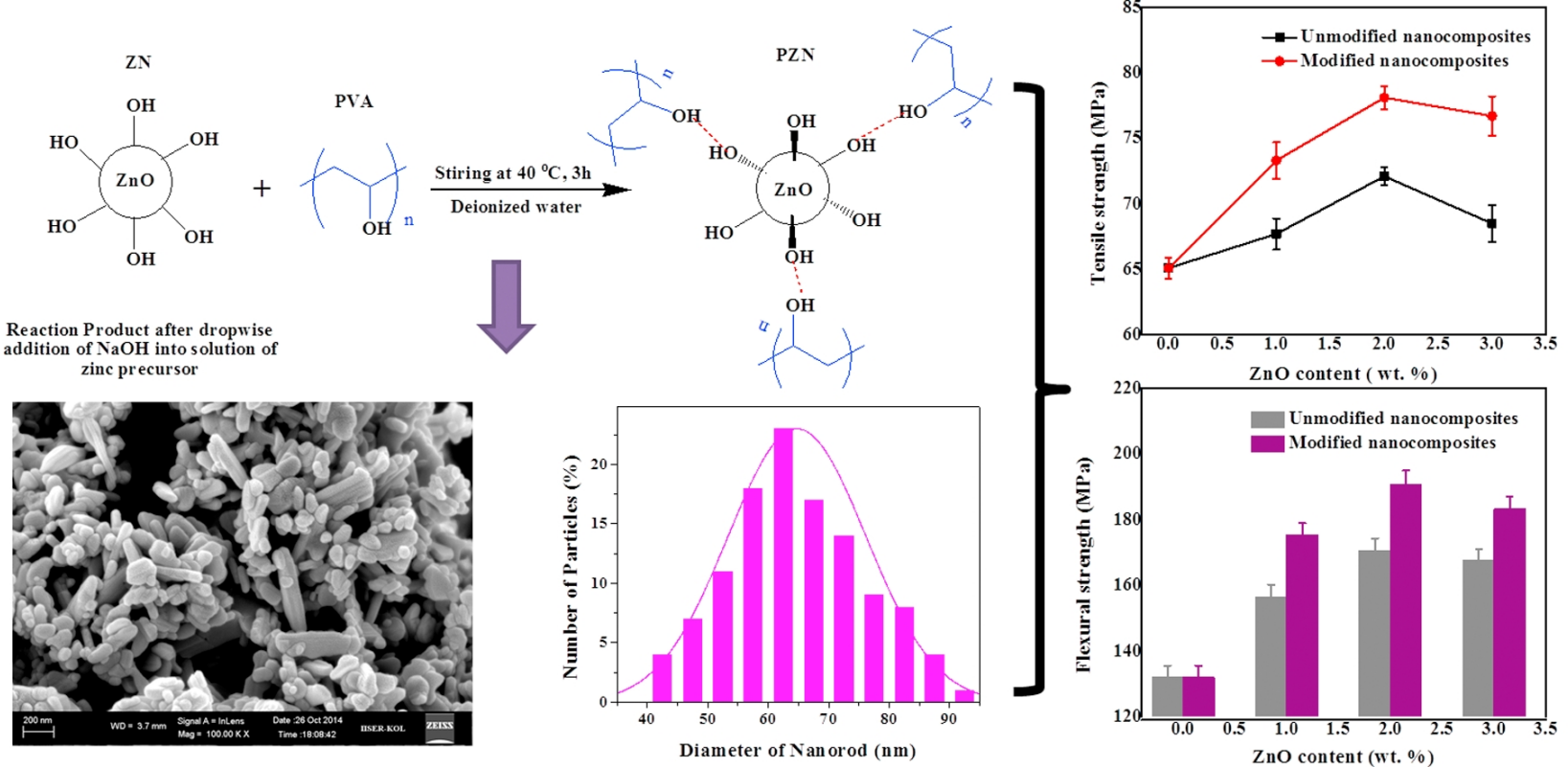
ZN
PVA
PZN
ZnO
OH
HO
Stiring at 40 °C, 3h
Deionized water
Reaction Product after dropwise addition of NaOH into solution of zinc precursor
200 nm
WD = 3.7 mm
Signal A = InLens
Mag = 100.00 K X
Date :26 Oct 2014
Time :18:08:42
IISER-KOL
ZEISS
Number of Particles (%)
Diameter of Nanorod (nm)
Unmodified nanocomposites
Modified nanocomposites
Tensile strength (MPa)
ZnO content (wt. %)
Flexural strength (MPa)
ZnO content (wt. %)